SRTTU

JCARME
ISSN: 2228-7922
Journal of Computational and Applied Research in Mechanical Engineering
Vol. 10, No. 1, pp. 51-62
jcarme.sru.ac.ir

Transient analysis of radiative hydromagnetic poiseuille fluid flow of two-step exothermic chemical reaction through a porous channel with convective cooling

S. O. Salawu[a,*], A. Abolarinwa[a] and O. J. Fenuga[b]

[a]*Department of Mathematics, Landmark University, Omu-aran, Nigeria.*

[b]*Department of Mathematics, University of Lagos, Lagos, Nigeria.*

Article info:

Type: Research
Received: 13/08/2018
Revised: 20/05/2019
Accepted: 26/052019
Online: 26/05/2019

Keywords:

Radiation,
Hydromagnetic,
Poiseuille flow,
Exothermic reaction,
Convective cooling.

Abstract

In this research, the transient analysis of radiative combustible viscous chemical reactive two-step exothermic fluid flow past a permeable medium with various kinetics, i.e., bimolecular, Arrhenius, and sensitized, are investigated. The hydromagnetic liquid is influenced by periodic vicissitudes in the axial pressure gradient and time along the channel axis in the occurrence of walls asymmetric convective cooling. The convectional heat transport at the wall surfaces with the neighboring space takes after the cooling law. The non-dimensional principal flow equations are computationally solved by applying convergent and absolutely stable semi-implicit finite difference techniques. The influences of the fluid terms associated with the momentum and energy equations are graphically presented and discussed quantitatively. The results show that the reaction parameter is very sensitive, and it, therefore, needs to be carefully monitored to avoid systems blow up. Also, a rise in the values of the second step term enhances the combustion rate and thereby reduces the release of unburned hydrocarbon that polluted the environment.

1. Introduction

In fluid mechanics, Poiseuille flow is a viscous and laminar fluid flow in the space within fixed surfaces. Poiseuille flow arises in fluid mechanism without motioning parts. If the plate surfaces are flat and smooth with unchanged liquid characteristics, it result in the linear simple flow profile, with a drag inversely relative to the gap width and proportionate to the relative velocity [1-4]. In several machines, operation and technology units under diverse circumstances need different types of lubricants. Commonly, lubricating oils viscosity frequently reduces with a rise in temperature. The difference in viscosity of the lubricant definitely impacts its efficiency. To circumvent unwanted changes in viscosity owing to the heat, the study of magnetic field and conducting liquids has appealed to numerous scientists which include [5-9]. Electrical and high thermal conductivity is attributed to hydromagnetic lubricants with lesser viscosity than the conventional lubricating oils. The heat produced by viscous friction is freely conducted away with high thermal conductivity, but lower viscous property reduces the amount of load-carrying that in turn affects

[*]*Corresponding author*
email address: kunlesalawu2@gmail.com

the electrical conducting of the fluid, which is possibly enhanced by applying electromagnetic fields externally. Nevertheless, ohmic heating as a result of electrical current raises the lubricant viscosity. Many studies on the hydrodynamic of lubricants in bearing cases have been established as it can be seen in examining the magnetic effects on hydrostatic bearing [10, 11].

The study of hydromagnetic reactive fluid past porous media with small Reynold's number in the occurrence of heat radiation has long remained a subject of discussion in the area of environmental science, biomedical, chemical science, and engineering. Also in extrusion of polymer, groundwater movement, nuclear reactor design, etc. in line with its usefulness, the radiation impacts on the convection MHD flow over permeable surface occupied with porous media were investigated by different researchers [12, 13]. The studied of radiative hydromagnetic fluid flow through walls considering the consequence of energy and species transport on the flow was examined by Makinde [14, 15]. While Kareem and Salawu [6] studied radiative oscillatory viscous mixed convection current carry liquid. Analysis of thermal runaway of convective boundary layers in a saturated viscous reactive flow liquid past a permeable channel was examined by Salawu and Oke [16] and Makinde [17]. Meanwhile, internal heating of a combustible materials result in an impulsive eruption such as manufacturing wool waste, fuel waste and coal waste maybe seen as heat explosion materials [18-21]. In fact, assessment of the main regimes through a regime splitting the area of criticality and non-criticality reactions is the core theory of ignition [22-25]. Frank- Kamenestkii [24] initiated the mathematical setup for the explosion model. The essentials of a two-step exothermic combustion system can not be overstressed as a result of its assistance in aiding complete hydrocarbon ignition is a system developed by Szabo [26]. The process supports the reduction of toxic discharge from the automobile engines that contaminant the atmosphere. In a slab, The exothermic reaction of second step thermal stability was reported by Makinde et al. [27].

The authors examined the diffusion reactant by taking the pre-exponential variable index for steady and unsteady state into consideration. Recently, the problem of an unsteady radiative two-step exothermic chemical combustible, viscous, reactive flowing fluid past porous media with various kinetics was investigated [28, 29]. The authors got results of the problem by coupled differential and Laplace transform.

In this study, the core concern in the analysis is to investigate the flow transient incompressible hydromagnetic fluid of a second step reaction moving past fixed walls with asymmetric convective cooling and uniform transverse magnetic field under diverse kinetics.

2. Model formulation

Examining the incompressible transient viscous flow in exothermic reactive hydromagnetic of step two is taken place within static parallel plates of width α. The flow is enhanced by the influence of bimolecular chemical kinetic and pressure. The flow is controlled by magnetic fieldB_0 applied externally. The upper and lower surface of the plates are open to exchange temperature with the surrounding heat. The x-axis is taken towards the center of the wall, while the y-axis is assumed normal to it. The flow geometry is presented in Fig. 1 and the model equations controlling the velocity and heat are given in Eqs. (1) and (2).

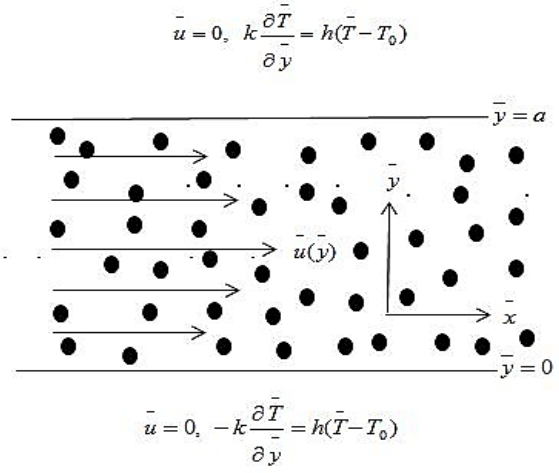

Fig. 1. The formulation geometry.

$$\rho\frac{\partial\bar{u}}{\partial\bar{t}}=-\frac{\partial\bar{P}}{\partial\bar{x}}+\mu\frac{\partial^2\bar{u}}{\partial\bar{y}^2}-\sigma B_0^2\bar{u}-\frac{\mu\bar{u}}{K_1} \quad (1)$$

$$\rho C_p\frac{\partial\bar{T}}{\partial\bar{t}}=k\frac{\partial^2\bar{T}}{\partial\bar{y}^2}-\frac{\partial q}{\partial\bar{y}}+\mu\left(\frac{\partial\bar{u}}{\partial\bar{y}}\right)^2+$$
$$Q_1C_1A_1\left(\frac{k\bar{T}}{\nu l}\right)^m e^{\frac{E_1}{R\bar{T}}}+Q_2C_2A_2\left(\frac{k\bar{T}}{\nu l}\right)^m e^{\frac{E_2}{R\bar{T}}}$$
$$+\frac{\mu\bar{u}^2}{K_1}+\sigma B_0^2\bar{u}^2+Q_0\left(\bar{T}-T_w\right) \quad (2)$$

with applicable boundary conditions of:

$$\begin{aligned}&\bar{u}(a,\bar{t})=0,\ \bar{u}(\bar{y},0)=0,\\&\bar{u}(0,\bar{t})=0,\ \bar{T}(\bar{y},0)=T_0,\\&-k\frac{\partial\bar{T}}{\partial\bar{y}}(0,\bar{t})=h\left(\bar{T}(0,\bar{t})-T_0\right),\\&k\frac{\partial\bar{T}}{\partial\bar{y}}(a,\bar{t})=h\left(\bar{T}(a,\bar{t})-T_0\right)\end{aligned} \quad (3)$$

the subsequent non-dimensional variables are applied as:

$$\begin{aligned}&y=\frac{\bar{y}}{a},\ x=\frac{\bar{x}}{a},\ T=\frac{E_1\left(\bar{T}-T_w\right)}{RT_w^2},\ G=-\frac{\partial p}{\partial x},\\&P=\frac{a\bar{p}}{\mu U},\ H^2=\frac{\sigma B_0^2a^2}{\mu},\ \varepsilon=\frac{RT_w}{E_1},\ r=\frac{E_2}{E_1},\\&u=\frac{\bar{u}}{U},\ Br=\frac{\mu U^2E_1}{kRT_w^2},\ T_a=\frac{E_1\left(T_0-T_w\right)}{RT_w^2},\\&\lambda=\frac{Q_1C_1A_1E_1a^2}{kRT_w^2}\left(\frac{kT_w}{\nu l}\right)^m e^{\frac{1}{\varepsilon}},\ t=\frac{\mu\bar{t}}{\rho a^2},\\&\beta=\frac{Q_0RT_w^2}{Q_1C_1A_1E_1}\left(\frac{kT_w}{\nu l}\right)^m e^{-\frac{1}{\varepsilon}},\ \varphi=\frac{a^2}{K_1},\\&\gamma=\frac{Q_2C_2A_2}{Q_1C_1A_1},\ \mathrm{Pr}=\frac{\mu C_p}{k},\ R_a=\frac{4\delta T_\infty}{ka_r}.\end{aligned} \quad (4)$$

Following Rosseland approximation discussed by Salawu and Fatunmbi [10], the directional heat radiative flux can be modeled in the form of:

$$q=-\frac{4\delta}{3a_r}\frac{\partial T^4}{\partial\bar{y}}, \quad (5)$$

where a_r is the absorption mean coefficient. If the heat difference in the liquid is of lower quantity, T^4 takes the linear temperature arrangement form. Therefore, Taylor series expansion of T^4 for about T_∞, with ignoring greater order terms, is

$$T^4=4T_\infty^3-3T_\infty^4 \quad (6)$$

Using the dimensionless parameters of Eq. (4) along with Eqs. (5) and (6) on Eqs. (1-3), the following equation is obtained:

$$\frac{\partial u}{\partial t}=G+\frac{\partial^2u}{\partial y^2}-H^2u-\varphi u \quad (7)$$

$$pr\frac{\partial T}{\partial t}=\left(1+\frac{4}{3}R_a\right)\frac{\partial^2T}{\partial y^2}+$$
$$Br\left[\left(\frac{\partial u}{\partial y}\right)^2+\left(H^2+\varphi\right)u^2\right]+ \quad (8)$$
$$\lambda\left[\left(1+\varepsilon T\right)^m\left(e^{\frac{T}{1+\varepsilon T}}+\gamma e^{\frac{rT}{1+\varepsilon T}}\right)+\beta T\right]$$

the resultant conditions is transformed to:

$$\begin{aligned}&u(y,0)=0,\ u(1,t)=0,\ u(0,t)=0,\\&T(y,0)=T_a,\ \frac{\partial T}{\partial y}(0,t)=-BiT(0,t),\\&\frac{\partial T}{\partial y}(1,t)=BiT(1,t)\end{aligned} \quad (9)$$

Other dimensionless equations of concern are the wall fluid friction (C_f), and wall temperature gradient (Nu) gotten as:

$$C_f=\frac{du}{dy}(1,t),\ Nu=-\frac{dT}{dy}(1,t) \quad (10)$$

Therefore, Eqs. (7) to (10) are computationally solved by the adopted numerical scheme.

3. Method of solution

The numerical procedure involved in the velocity and heat equations is finite-difference of semi-implicit kind given in references [30, 31]. The method assumes implicit terms in-between the interval space $(\xi + N)$ for $1 \geq \xi \geq 0$. To make large interval sizes, ξ is assumed to be 1. Actually, being completely implicit, the embraced computational procedure utilized in this study is postulated to be suitable for all forms of interval sizes. The equations are discretized on a linear Cartesian mesh with unvarying grid in which the finite differences are defined. Approximate the spatial main and succeeding derivatives with second order central differences, the boundary conditions following the first and last grid points used is integrated. The velocity component can be express as follows:

$$\frac{\left(u^{(N+1)} - u^{(N)}\right)}{\Delta t} = -\varphi u^{(N+\xi)} + u_{yy}^{(N+\xi)} + G - H^2 u^{(N+\xi)} \quad (11)$$

The equation for $u^{(N+1)}$ takes the form:

$$-b_1 u_{j-1}^{N+1} + \left[1 + 2b_1 + \left(H^2 + \varphi\right)\Delta t\right] u_j^{N+1} - b_1 u_{j+1}^{N+1} = u^{(N)} + \Delta t(1-\xi) u_{yy}^{(N)} + \Delta t G - \Delta t\left(\varphi + H^2\right)(1-\xi) u^{(N)} \quad (12)$$

where $b_1 = \xi \Delta t / \Delta y^2$ and the derivatives of time in forwarding difference schemes are taken. Therfore, the $u^{(N+1)}$ solution scheme changes to matices of tri-diagonal inversion.

The semi-implicit expression for heat equation takes after the flow rate equation defined. Hence, the heat derivatives for the second-order is expressed as:

$$\mathrm{Pr}\frac{T^{(N+1)} - T^{(N)}}{\Delta t} = \left(1 + \frac{4}{3} R_a\right)\frac{\partial^2 T^{(N+\xi)}}{\partial y^2} + Br\left[u_y^2 + \left(H^2 + \varphi\right)u\right]^{(N)} + \lambda\left[\left(1 + \varepsilon T\right)^m \left(e^{\frac{T}{1+\varepsilon T}} + \gamma e^{\frac{rT}{1+\varepsilon T}}\right) + \beta T\right]^{(N)} \quad (13)$$

Then $T^{(N+1)}$ is translated to:

$$-b_2 T_{j-1}^{(N+1)} + \left(\mathrm{Pr} + 2b_2\right) T_j^{(N+1)} - b_2 T_{j+1}^{(N+1)} = T^{(N)} + \Delta t(1-\xi)\left(1 + \frac{4}{3} R_a\right) T_{yy}^{(N)} + Br\Delta t\left[u_y^2 + \left(H^2 + \varphi\right)u\right]^{(N)} + \lambda\Delta t\left[\left(1 + \varepsilon T\right)^m \left(e^{\frac{T}{1+\varepsilon T}} + \gamma e^{\frac{rT}{1+\varepsilon T}}\right) + \beta T\right]^{(N)} \quad (14)$$

where $b_2 = \xi \Delta t / \Delta y^2$. Also, the scheme system for $T^{(N+1)}$ reduces to inversion tridiagonal matrices. The systems of Eq. (9) and Eq. (11) are confirmed for regularity when $\xi = 1$ allowing large interval sizes of order two in level, but exact in order one. As formerly taken, the method satisfies all forms of values in time! Maple software is adopted for computational solutions.

6. Results and discussion

The initial reactive liquid temperature is assumed to equal to the heat at the wall, hence the term $T_a = 0$. The following default parameters $\varphi = 0.2$, $Br = 1$, $G = 1$, $m = 0.5$, $Pr = 7.0$, $\lambda = 2$, $r = 1$, $\gamma = 1$, $t = 5$, $R_a = 0.5$, $\varepsilon = 1$, $H = 1$, and $\beta = 0.5$ are used based on existing theoretical research except otherwise stated on the graph. Table 1 denotes the significance of emerging fluid terms on the reactive two-step heat criticality. A rise in the terms γ, Br, Q, and r reduces the Frank-Kamenettski critical values (λ_c) due to the fact that the term causes delineation in the heat boundary layer. This leads to rises in the heat diffusing out of the system, but the revised is the case with a rise in the term φ that results in enhancement of Frank-Kamenettski's critical values (λ_c). It is because the term influences the rise in the temperature of the system. The term λ is a strong heat enhancement, and it needs to be carefully managed and guide because high values of the term can cause solutions to blow up as seen in the table.

Table 2 presents the system of thermal ignition with bimolecular kinetic occurs quicker than

Arrhenius and senstitized kinetics. This is because the bimolecular reaction is assumed with lower heat criticality value. A significant rise is observed in the heat ignition with a decline in the activation energy, hence heat stability is encouraged with early decrease in the thermal runaway.

The transient solutions for momentum and energy distributions with finer even mesh ($\Delta t = 0.001$ with $\Delta y = 0.001$) are presented in Figs. 2 and 3. The plots denote a steady rise in both the momentum and heat transfer rate utill it reaches a stable state. Therefore, as time increases the flow and energy transfer rates in the channel are encouraged.

Fig. 4 denotes the temperature blow up for huge values of λ. It is important to note that depending on certain parameters values under consideration, the stable momentum and temperature fields, as demostrated in Figs. 2 and 3, may be difficult to achieve.

Most especially, the reaction term λ, which needs cautious manage and guide, can create solutions inflatable, as displayed in Fig. 4, because of the large values. As depicted in the plot, the parameter λ is related to high heat source.

Fig. 5 represents the impact of differences in the values of pressure gradient G on the momentum fields. A boost in the values of pressure gradient enhances the flow rate in the system, that is the highest velocity experienced as the parameter values G increase, inferring that the enormous the pressure introduced on the liquid flow in a channel, the quicker the flow as a result of warmth in the fluid as the pressure increases.

Table 1. The solutions criticality for various emerging terms.

Br	r	Bi	G	H	γ	φ	R_a	β	m	ε	λ_c
0.5	2.0	1.0	1.0	1.0	1.0	0.1	0.5	0.5	0.5	0.5	0.06543286595758994
0.5	3.0	1.0	1.0	1.0	1.0	0.1	0.5	0.5	0.5	0.5	0.02643637641373641
0.5	1.0	1.0	1.0	1.0	1.0	0.1	0.5	0.5	0.5	0.5	0.14307817321101074
0.5	1.0	1.0	1.0	1.0	2.0	0.1	0.5	0.5	0.5	0.5	0.08463136436821836
0.5	1.0	1.0	1.0	1.0	1.0	0.2	0.5	0.5	0.5	0.5	0.14316085047224741
0.5	1.0	1.0	1.0	1.0	1.0	0.3	0.5	0.5	0.5	0.5	0.14324120784003946
0.5	1.0	2.0	1.0	1.0	1.0	0.1	0.5	0.5	0.5	0.5	0.13900376624897837
0.5	1.0	3.0	1.0	1.0	1.0	0.1	0.5	0.5	0.5	0.5	0.13519246785211794
0.5	1.0	1.0	1.0	1.0	1.0	0.1	0.0	1.0	0.5	0.5	0.13558848416143185
0.5	1.0	1.0	1.0	1.0	1.0	0.1	0.5	1.5	0.5	0.5	0.12885813171589758

Table 2. Comparison of numerical values for thermal explosion with various kinetics of $Br = R = G = \varphi = \beta = G = Bi = H = 0, Pr = 1$.

				Makinde et al. (2015)		Current results	
ε	r	m	γ	θ_{max}	λ_c	θ_{max}	λ_c
0.1	0.1	0.5	0.0	1.420243875	0.932216072	1.420244002	0.932216754
0.1	0.1	0.5	0.1	1.476474346	0.897649656	1.476473998	0.897648864
0.1	0.1	0.5	0.2	1.5294654+	0.866522770	1.529465722	0.866523029
0.1	0.1	0.0	0.1	1.585899049	0.953645221	1.585898894	0.953644916
0.1	0.1	-0.2	0.1	2.320778138	1.282091040	2.320777965	1.282099988
0.1	0.5	0.5	0.1	1.467926747	0.880606329	1.467927112	0.880606809
0.1	1.0	0.5	0.1	1.420243875	0.847469156	1.420244097	0.847469561
0.2	0.1	0.5	0.1	1.905274235	0.968086041	1.905273899	0.968085638
0.3	0.1	0.5	0.1	3.046841932	1.074421454	3.046842131	1.074422119

Fig. 6 depicts the influence of diverse values of Hartmann number H on the fluid momentum. It is noticed that increasing the values of magnetic field term H enhances the magnetic damping properties because of the existence of the Lorentz force that leads to amplification of the flow liquid resistance; thereby, slows down the reactive liquid motion.

Accordingly, the conducting fluid is driven by the magnetic force, hence the fluid flow micro-scale system is induced by electrical conductivity. Therefore, the velocity profile reduces. Fig. 7 illustrates the impact of Brinkman number Br on the energy field. It is seen that increasing the Brinkman number encourages the temperature field.

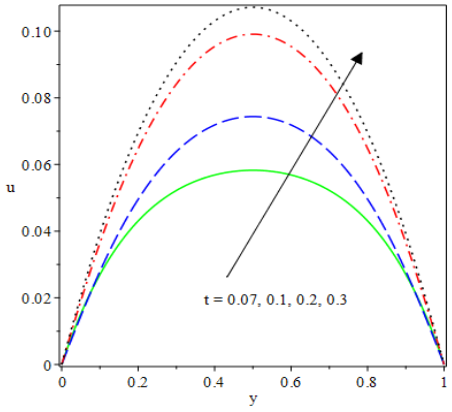

Fig. 2. Transient state velocity profile.

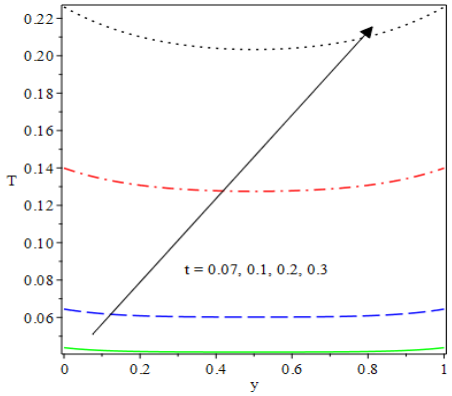

Fig. 3. Transient state temperature profile.

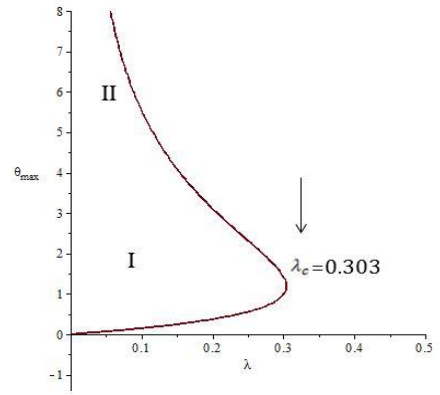

Fig. 4. Blow up bifurcation diagram for high λ.

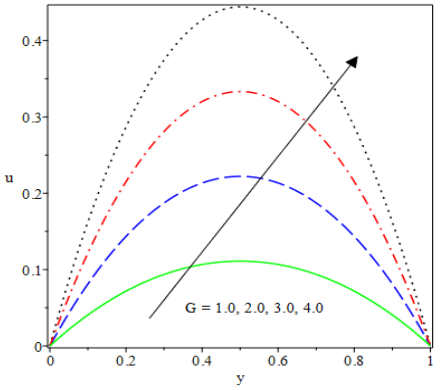

Fig. 5. Effects of G on velocity.

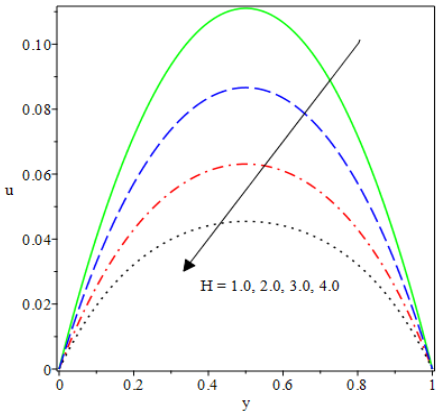

Fig. 6. Effects of (H) on velocity.

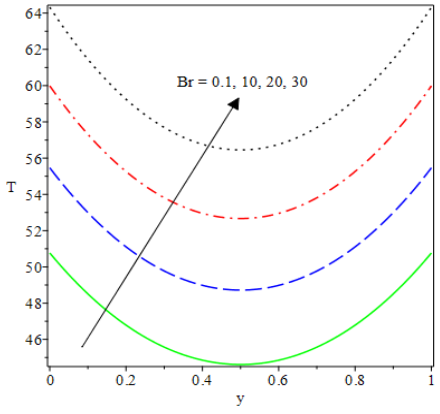

Fig. 7. Effects of (Br) on temperature.

The term Br is associated with ohmic heating in the temperature equation, consequently, higher Br values causes an enhancement in the temperature produced by the fluid shear stress causing a rise in the fluid energy within the system. Fig. 8 shows the consequence of changing the exothermic second step term values γ on the energy profiles. It is observed that a rise in values of γ results in a substantial increase in the energy profiles. This is due to rises in the thickness of the heat boundary layer as the values of γ are boosted. This then results in the reduction of the heat quantity, leaving the system, which in turn builds up the temperature field.

Fig. 9 confirms the influence of λ on the heat profile. An increase in the Frank-Kamenetskii term λ enhances the heat distributions in the system, which is against the role performed by the Prandtl number. Rising the values of λ brings about intensification in the reaction as well as the ohmic heating terms; thus absolutely enhances the flow liquid temperature as appeared in the figure. The momentous rises in the heat are because of the increment in the parameter λ, which implies that the momentum fluid viscosity is encouraged, consequently resulted in a rise in the heat field.

Fig. 10 portrays the influence of porosity parameter φ on the momentum profile. It is noticed from the plot that the flow fluid rate diminishes as the porosity term rises. This is because the surfaces of the plate provide a supportive resistance to the fluid flow mechanism and cause the reactive liquid to motion at a slow rate. The effect is significant because a boost in the porosity term values discourages heat source terms, thereby it reduces the rate of heat transfer within the system. The fluid particles collision rate diminishes, which then results in the overall reduction of the flow velocity, as seen in the diagram.

Figs. 11-13 independently show the response of the temperature field to differences in the kinetics m that is the bimolecular, Arrhenius, and sensitized, on an increase in the activation energy ε. It is obtained from the figures that a noteworthy diminishing in the reactive liquid heat as the values of the term ε rises for the bimolecular, Arrhenius, and sensitized kinetics, i.e., at $m = 0.5, 0, -2$. However, the term defines the source terms in the heat component.

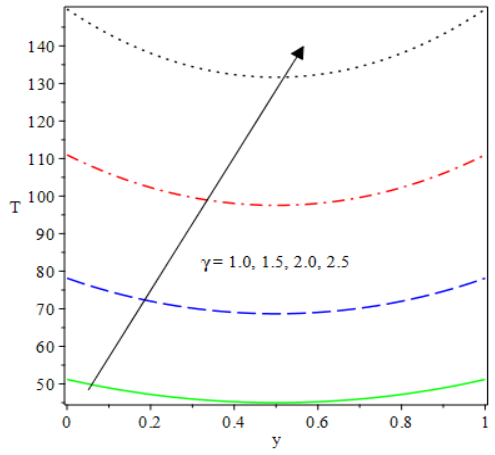

Fig. 8. Effects of (γ) on temperature.

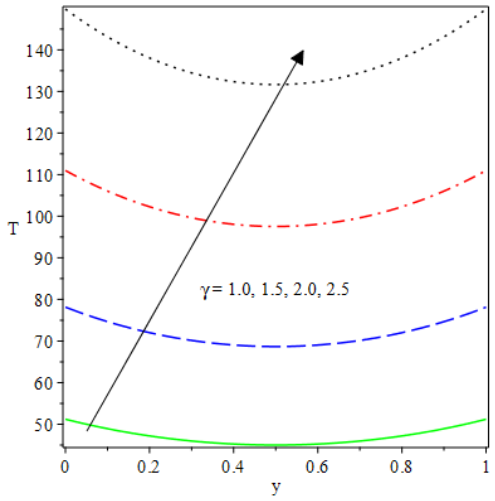

Fig. 9. Effects of λ on temperature.

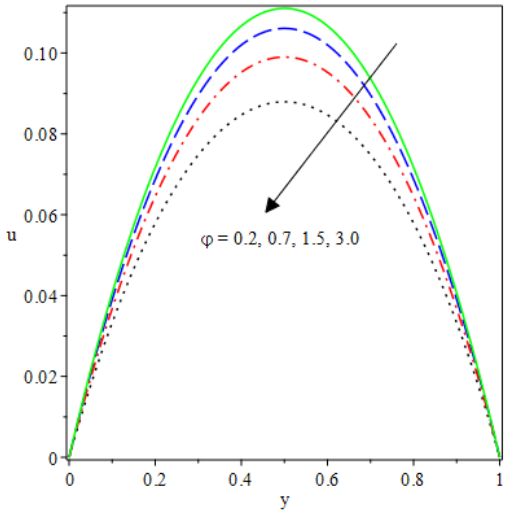

Fig. 10. Effects of φ on velocity.

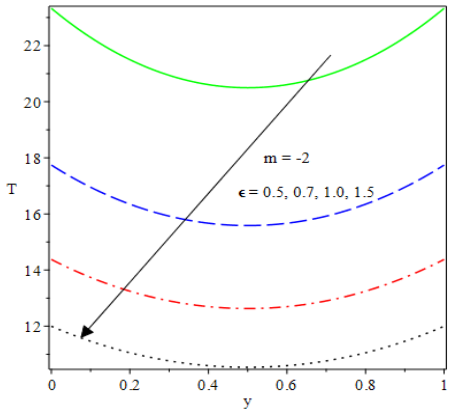

Fig. 11. Effects of ε on temperature when m =-2

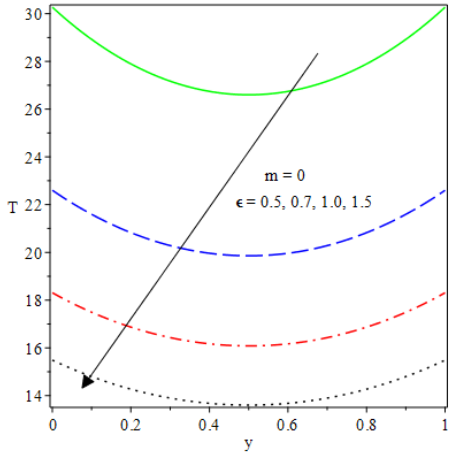

Fig. 12. Effects of ε on temperature when $m = 0$.

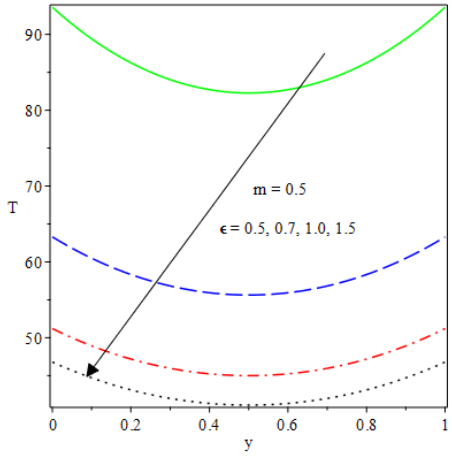

Fig. 13. Effects of ε on temperature when $m = 0.5$.

The influences of varying radiation on the energy distributions is reported in Fig. 14. It is noticed that as the parameter values of R increases, there are corresponding rises in the temperature profiles that lead to a rise in the thickness of the temperature boundary layer. The plot shows that a rise in the term R encourages the thickness of the temperature boundary layer that turns to enhance the heat field and slow down the coefficient of heat gradient at the wall. Fig. 15 illustrates the reaction of the fluid temperature to the variational rise in the heat generation parameter β. As noticed in the diagram, rising the heat source increases the heat distribution in the channel due to a rise in the temperature boundary layer that enhances the amount of heat within the chemical reactive system.

Figs. 16 and 17 portrays the difference in the wall shear stress with increasing in the term G values and Hartmann number H depending on the reaction term λ.

An early rise and fall are respectively noticed as the values of the terms G and H increase near the channel wall. But a revised in the behavior is observed as they respectively move far away from the wall at $\lambda \geq 0.5$ towards the free flow.

Figs. 18 and 19 represent the wall heat gradient rate with variational rises in the parameters value β and ε depending on the second-step exothermic chemical reaction term γ. Follow from the plots, a gradual rise in the wall heat gradient from a very lower state is seen between $0 \leq \gamma \leq 0.5$. While, a conversed behavior is obtained in the solutions at finite time temperature. Hence, the rate at which energy transfer in a two-step chemical reactive at the wall decreases at $\gamma \geq 0.5$ for free reactive flow.

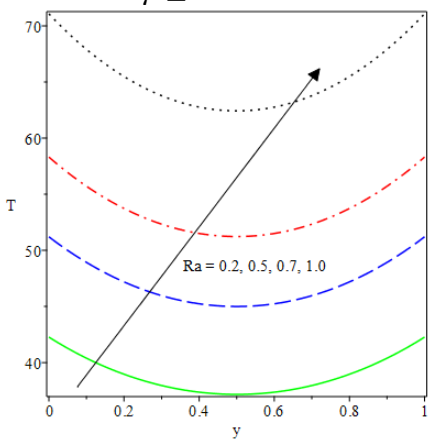

Fig. 14. Effects of Ra on temperature.

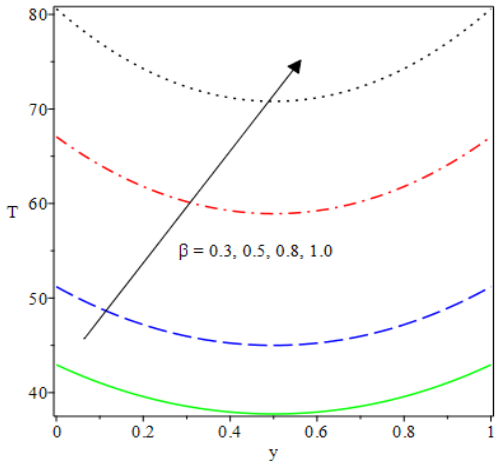

Fig. 15. Effects of (β) on velocity.

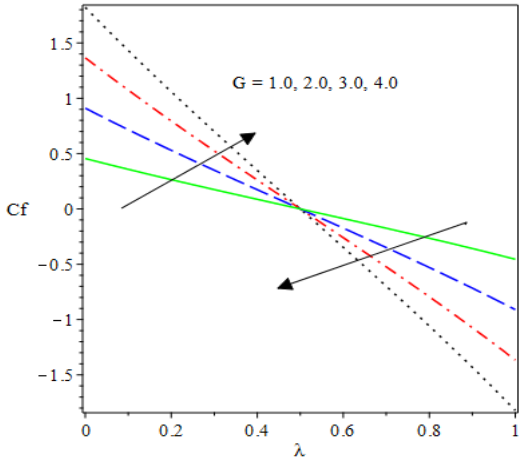

Fig. 16. Wall shear stress with variation in λ and G.

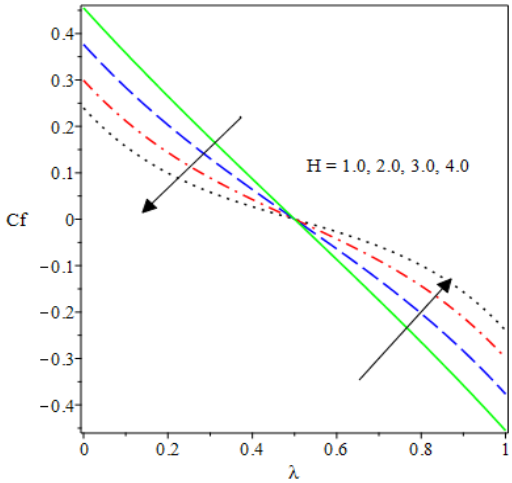

Fig. 17. Wall shear stress with variation in λ and H.

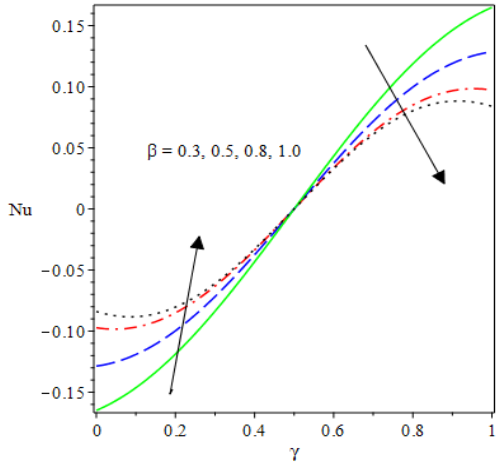

Fig 18. Wall heat transfer with vatiation in γ and β.

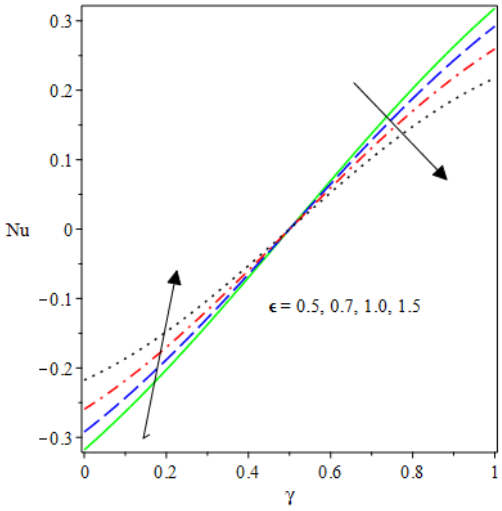

Fig. 19. Wall heat transfer with variation in γ and ε

4. Conclusions

The unsteady exothermic reactive two-step fluid flow passes permeable static channel with asymmetry convective cooling is examined in the presence of a magnetic field. The governing non-dimensional flow and energy equations are solved by applying a convergent and consistent finite-difference of the semi-implicit scheme. From the study, it is noticed that the heat content in the reactive system decreases for all the kinetics, i.e., the bimolecular, Arrhenius, and sensitized chemical kinetics for variational rises in the activation energy.

The decrease in the heat happens because the

heat source terms decrease as the activation energy term rises. The magnetic field reduces the flow, and it helps to avoid unwanted changes in the fluid viscosity as a result of high heat. The magnetic field effect is due to the the result of the Lorentz force that drags the reactive flow fluid. Eectrical and high thermal conductivity is credited to hydromagnetic lubricants with lesser viscosity than the conventional lubricant oils. Furthermore, reactive exothermic second step term γ shows a substantial increase in the heat distribution, which demostrates a total ignition of unburned hydrocarbon in the reaction system. Moreover, a small rise in the Frank-Kamenetskii term λ can cause thermal criticality. Hence, the reaction parameter λ is very sensitive to an increase, and it, therefore, needs to be carefully monitored to avoid blow-up of the solutions.

References

[1] A. Aziz, "Entropy generation in pressure gradient assisted Couette flow with different thermal boundary conditions", *Entropy*, Vol. 8, No. 2, pp. 50-62, (2006).

[2] G. K. Batchelor, *An Introduction to Fluid Dynamics*, Cambridge Mathematical Library. Cambridge University Press, Cambridge, Mass, USA, (1999).

[3] M. G. Reddy, M. V. V. N. L. Sudha Rani, K. G. Kumar, and B. C. Prasannakumara, "Cattaneo-Christov heat flux and non-uniform heat source/sink impacts on radiative Oldroyd-B two-phase flow across a cone/wedge", *Journal of the Brazilian Society of Mechanical Sciences and Engineering*, Vol. 40, p. 95, (2018).

[4] S. O. Salawu, and S. A. Amoo, "Effects of variable viscosity and thermal conductivity on dissipative heat and mass transfer of MHD flow in a porous medium", *Advance in multidispl. & Scientific Research (AIMS)*, Vol. 2, pp. 11-22, (2016).

[5] M. S. Dada, and S. O. Salawu, "Analysis of heat and mass transfer of an inclined magnetic field pressure-driven flow past a permeable plate", Applications and Applied Mathematics: *An International Journal*, Vol. 12, pp. 189-200, (2017).

[6] R. A. Kareem, and S. O.Salawu, "Variable viscosity and thermal conductivity effect of soret and dufour on inclined magnetic field in non-Darcy permeable medium with dissipation", *British Journal of Mathematics & Computer Science*, Vol. 22, pp.1-12, (2017).

[7] M. Malik, and D. V. Singh, "Analysis of finite magnetohydrodynamic", *journal bearings*, Wear, Vol. 64, No. 2, pp. 273-280, (1980).

[8] K. D. Singh, "Exact solution of MHD mixed convection periodic flow in a rotating vertical channel with heat radiation", *Int. Journal of Applied Mechanics and Engineering*, Vol. 18, No. 3, pp. 853-869, (2013).

[9] M. F. Dimian, and A. H. Essawy, "Magnetic field effects on mixed convection between rotating coaxial disk", *J. Engineering Physics and thermophysics*, Vol. 739, No. 5, pp. 1082-1091, (1999).

[10] S. O. Salawu, and E. O. Fatunmbi, "Dissipative heat transfer of micropolar hydromagnetic variable electric conductivity fluid past inclined plate with joule heating and non-uniform heat generation", Asian *Journal of Physical and Chemical Sciences*, Vol. 2, pp. 1-10, (2017).

[11] D. S. Chauhan, and P. Rastogi, "Radiation effects on natural convection MHD flow in a rotating vertical porous channel partially filled with a porous medium", *Applied Mathematical Sciences*, Vol. 4, No. 13, pp. 643-655, (2010).

[12] I. J. Uwanta, M. Sani, and M. O. Ibrahim, "MHD convection slip fluid flow with radiation and heat deposition in a channel in a porous medium", *International Journal of Computer Applications*, Vol. 36, No. 2, pp. 41-48, (2011).

[13] T. Hayat, M. Awais, A. Alsaedi, and A. Safdar, "On computations for thermal radiation in MHD channel flow with heat and mass transfer", *Plos one*, Vol. 9, No. 1, pp. 1-5, (2014).

[14] O. D. Makinde, "Thermal stability of a reactive viscous flow through a porous saturated channel with convective boundary conditions", Applied Thermal Engineering, Vol. 29, No. 8-9, pp. 1773-1777, (2009).

[15] O. D. Makinde, "Exothermic explosions in a slab: A case study of series summation technique, *International and Mass Transfer*, Vol. 31, No. 8, pp. 1227-1231, (2004).

[16] S. O. Salawu, and S. I. Oke, "Inherent irreversibility of exothermic chemical reactive third grade poiseuille flow of a variable viscosity with convective cooling", *J. Appl. Comput. Mech.*, Vol. 4, No. 3, pp. 167-174, (2018).

[17] O. D. Makinde, "Thermal criticality for a reactive gravity driven thin film flow of a third grade fluid with adiabatic free surface down an inclined plane ", *Applied Mathematics and Mechanics*, Vol. 30, No. 3, pp. 373-380 , (2009).

[18] M. G. Reddy, "Heat and mass transfer on magnetohydrodynamic peristaltic flow in porous media with partial slip", *Alexandria Engineering Journal*, Vol. 55, No. 2, pp. 1225-1234, (2016).

[19] A. J. Chamkha, "Unsteady MHD convective heat and mass transfer past a semi-infinite vertical permeable moving plate with heat absorption", *Int J Eng. Sci*, Vol. 42, No. 2, pp. 217-230 , (2004).

[20] M. G. Reddy, and O. D. Makinde, "MHD peristaltic transport of Jeffrey nanofluid in an asymmetric channel, *Journal of Molecular Liquids*", Vol. 223, pp. 1242-1248, (2016).

[21] S. O. Adesanya, J. A. Falade, S. Jangili, and O. Anwar Be´ g, "Irreversibility analysis for reactive third-grade fluid flow and heat transfer with convective wall cooling, *Alexandria Engineering Journal*, Vol. 56, No. 1, pp. 153-160, (2017).

[22] E. Balakrishnan, A. Swift, and G.C. Wake, "Critical values for some non-class A geometries in thermal ignition theory". *Math. Comput. Modell*., Vol 24, No. 8, pp. l-10, (1996).

[23] J. Bebernes, and D. Eberly, *Mathematical problems from combustion theory*. Springer Verlag, New York, (1989).

[24] D. A. Frank-Kamenettskii, *Diffusion and heat transfer in chemical kinetics*. Plenum press, New York, (1969).

[25] A. R. Hassan, and R. Maritz, "The analysis of a reactive hydromagnetic internal heat generating poiseuille fluid flow through a channel", Springer Plus, Vol. 5, No. 1, pp. 2-14, (2016).

[26] Z. G. Szabo, *Advances in kinetics of homogeneous gas reactions*. Methusen and Co Ltd, Great Britain, (1964*)*.

[27] O. D. Makinde, P. O. Olanrewaju, E. O. Titiloye, and A.W. Ogunsola, "On thermal stability of a two-step exothermic chemical reaction in a slab", *Journal of Mathematical sciences*, Vol. 13, pp.1-15, (2013).

[28] R. A. Kareem, and J. A. Gbadeyan, "Unsteady radiative hydromagnetic internal heat generation fluid flow through a porous channel of a two-step exothermic chemical reaction", *Journal of Nig. Ass. of Math. Physics*, Vol. 34, pp.111-124, (2016).

[29] S. O. Salawu, N. K. Oladejo and M. S. Dada, "Analysis of unsteady viscous dissipative poiseuille fluid flow of two-step exothermic chemical reaction through a porous channel with convective cooling. Ain Sham Journal of Engineering. (2019).

[30] S. O. Salawu, and A. M. okedoye, "Thermodynamic second law analysis of hydromagnetic gravity-driven two-step exothermic chemical reactive flow with heat absorption along a Channel", *Iranian Journal of Energy and Environment*, Vol. 9, No. 2, pp. 114-120, (2018).

[31] O. D. Makinde, and T. Chinyoka, "Numerical study of unsteady hydromagnetic generalized couette flow of a reactive third-grade fluid with asymmetric convective cooling", Computer and Mathematics with Applications, Vol. 61, No. 4, pp. 1167-1179, (2011).

How to cite this paper:

S. O. Salawu, A. Abolarinwa and O. J. Fenuga, *"*Transient analysis of radiative hydromagnetic poiseuille fluid flow of two-step exothermic chemical reaction through a porous channel with convective cooling*", Journal of Computational and Applied Research in Mechanical Engineering*, Vol. 10, No. 1, pp. 51-62, (2020).

DOI: 10.22061/jcarme.2019.3986.1473

URL: http://jcarme.sru.ac.ir/?_action=showPDF&article=1056